View Article Online / Journal Homepage / Table of Contents for this issue

PAPER

NJC www.rsc.org/njc

Novel supramolecular charge-transfer systems based on bis(18-crown-6)stilbene and viologen analogues bearing two ammonioalkyl groups†

Sergey P. Gromov,*[a] Artem I. Vedernikov,[a] Evgeny N. Ushakov,[b] Natalia A. Lobova,[a] Asya A. Botsmanova,[a] Lyudmila G. Kuz'mina,[c] Andrei V. Churakov,[c] Yuri A. Strelenko,[d] Michael V. Alfimov,[a] Judith A. K. Howard,[e] Dan Johnels[f] and Ulf G. Edlund*[f]

[a] *Photochemistry Center, Russian Academy of Sciences, 7A Novatorov str., 119421 Moscow, Russian Federation. E-mail: gromov@photonics.ru; Fax: +7-095-9361255*
[b] *Institute of Problems of Chemical Physics, Russian Academy of Sciences, Chernogolovka, 142432 Moscow Region, Russian Federation*
[c] *N. S. Kurnakov Institute of General and Inorganic Chemistry, Russian Academy of Sciences, 31 Leninskiy prosp., 117907 Moscow, Russian Federation*
[d] *N. D. Zelinskiy Institute of Organic Chemistry, Russian Academy of Sciences, 47 Leninskiy prosp., 117913 Moscow, Russian Federation*
[e] *Chemistry Department, Durham University, South Road, Durham, UK DH1 3LE*
[f] *Department of Organic Chemistry, Umeå University, SE-901 87 Umeå, Sweden. E-mail: Ulf.Edlund@chem.umu.se; Fax: +46-90-7867844*

Received (in Montpellier, France) 17th January 2005, Accepted 24th March 2005
First published as an Advance Article on the web 11th May 2005

Downloaded by University of California - Los Angeles on 01 January 2013
Published on 11 May 2005 on http://pubs.rsc.org | doi:10.1039/B500667H

A series of new viologen analogues bearing two ammonioalkyl groups (**2–4**) were synthesized in order to study their complexation with bis(18-crown-6)stilbene (**1b**). Electronic spectroscopy and ^{1}H NMR measurements show that in acetonitrile, bis(crown) stilbene **1b** forms highly stable 1 : 1 and 2 : 1 charge-transfer (CT) complexes with π-acceptors **2–4** owing to host–guest bonding. The influence of geometric and electronic factors on the complex formation constants are discussed. The structures of the supramolecular CT complexes are analyzed on the basis of ^{1}H and ^{13}C NMR data obtained in solution and in the solid state. X-Ray diffraction data for **1b** and for model tetramethoxystilbene are also reported.

Introduction

Crown ethers are widely utilized as efficient polydentate ligands for metal and ammonium ions.[1] Supramolecular systems combining crown ethers and light-absorbing groups attract considerable attention as they have a potential for use in optical sensors for metal ions[2] and in photoswitchable molecular devices.[3] Functional groups whose spectroscopic characteristics are controlled by photophysical phenomena,[2b] such as photoinduced internal charge transfer, photoinduced electron transfer, excimer formation or electronic energy transfer are used as signalling moieties in crown ether-based optical sensors. The photoswitchable crown compounds are created using functional groups that can undergo substantial structural changes under the action of light.[4]

Recently,[5] we proposed a new type of photosensitive crown compound represented by a supramolecular complex between bis(18-crown-6)stilbene (**1b**, Scheme 1) and 1,2-bis[1-(3-ammoniopropyl)-4-pyridiniumyl]ethylene tetraperchlorate (**2b**, Scheme 2). This non-fluorescent complex shows a broad absorption band in the visible region, indicative of charge transfer in the ground state. Unlike usual organic donor (D)–acceptor (A) complexes,[6] this complex has a very high thermodynamic stability that is provided by two-centre host–guest bonding. It was demonstrated that the supramolecular complex between **1b** and **2b** can act as optical sensor for metal ions in non-aqueous environments.[5a] More recently, it was shown that under certain conditions, **1b** and **2b** can form a relatively stable 2(D) : 1(A) complex.[5b]

Here we report the first synthesis and results of a comprehensive study of new bi- and termolecular complexes composed of bis(crown) stilbene **1b** and diammonium π-acceptor salts **2c**, **3b** (Scheme 2) and **4b** (Scheme 3). The composition and the thermodynamic stability of these supramolecular systems and a number of model complexes in acetonitrile were determined by electronic spectroscopy and ^{1}H NMR titration. The structures

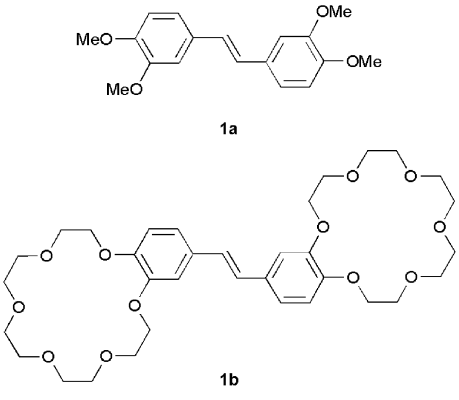

1a

1b

Scheme 1 Structure of donors **1a** and **1b**.

† Electronic supplementary information (ESI) available: Selected bond lengths and angles; solution and solid state ^{13}C NMR data for **1b**, **2b**, [**1b** · **2b**] and [(**1b**)$_2$ · **2b**]. See http://www.rsc.org/suppdata/nj/b5/b500667h/

DOI: 10.1039/b500667h

View Article Online

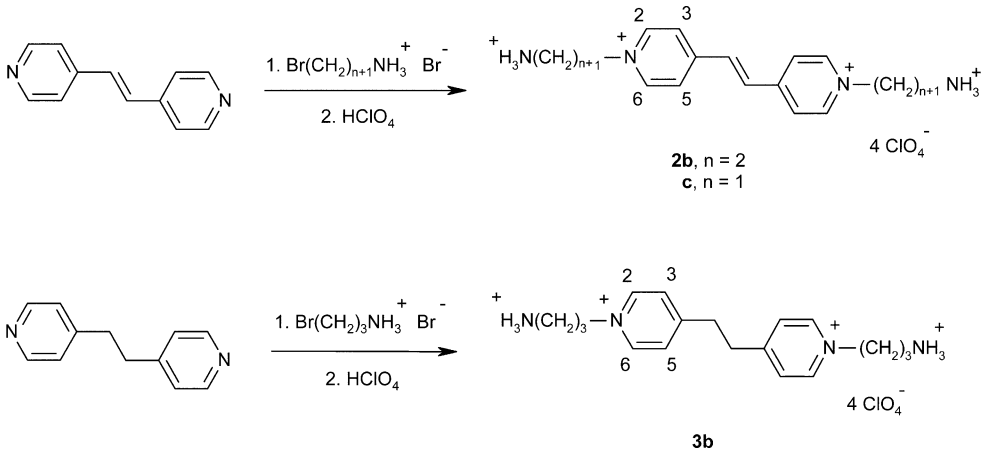

Scheme 2 Synthesis of acceptors **2b, c** and **3b**.

Downloaded by University of California - Los Angeles on 01 January 2013
Published on 11 May 2005 on http://pubs.rsc.org | doi:10.1039/B500667H

of the complexes in solution and in the solid state were studied by ^{1}H and ^{13}C NMR spectroscopy, including 2D COSY and NOESY techniques. For **1b** and 3,4,3′,4′-tetramethoxystilbene (**1a**, Scheme 1), X-ray diffraction data are presented.

Results and discussion

A. Synthesis

The synthesis of bis(crown) stilbene **1b** has been previously described in the literature and is based on the condensation of 4′-formylbenzo-18-crown-6 ether in the presence of Ti(III) salts; the yield of **1b** under these conditions was 31%.[7] When we replaced the drastic cooling at the preparation step of the tetrahydrofuran–titanium(IV) chloride complex by cooling to 0 °C, the yield of **1b** increased to 40%. The reference π-donor **1a**[7] was prepared under the same conditions in 59% yield. The electron-donating effect of the crown-ether fragments is mimicked by four methoxy groups in **1a**, but the formation of host–guest complexes is impossible. According to ^{1}H NMR data, stilbenes **1a, b** were formed as *E*-isomers.

The diammonium π-acceptor salts **2b, c** were synthesized by quaternization of (*E*)-di(4-pyridyl)ethylene with ω-bromoalkylamine salts in acetonitrile followed by replacement of bromide ions by perchlorate ions (Scheme 2, yields are 72% for **2b** and 29% for **2c**).

Similar procedures were used to synthesize the analogues of **2b** with a reduced π-acceptor strength, *i.e.*, **3b** with a central dimethylene chain, and bis-quaternary salt **4b** in which the pyridine residues are linked by an ethylene bridge through the β-positions. The key reactant for the synthesis of **4b**, (*E*)-di(3-pyridyl)ethylene [(*E*)-**7**], was unavailable, and the methods for its preparation described in the literature were either irreproducible or required the use of reagents difficult to prepare and rigorous reaction conditions.[8] Therefore we developed an alternative synthesis of (*E*)-**7** with Wittig condensation as the key step (Scheme 3).

In addition, we synthesized a few reference acceptor salts, **2a–4a** (Scheme 4) and **8** (Scheme 5), in order to study their complexation with **1b**. Compounds **2a–4a** are readily obtained by fusing together the appropriate heterocyclic bases with ethyl tosylate followed by treatment with perchloric acid.[9] Compound **8** was prepared using the synthetic procedure developed for **2b–4b**.

B. X-Ray diffraction studies

The molecular structures of **1a** and **1b** were determined by X-ray diffraction analysis. Two views of the molecules are shown in Fig. 1 and selected bond lengths and angles are listed in the ESI.†

Both molecules are situated at symmetry centres, their *E*-stilbene fragments being strictly planar. The conjugation of π-electrons over both the benzene rings and the double bond between them is decreased as indicated by the C(1)–C(2) and C(1)–C(1A) bond lengths (1.467(2) and 1.338(3), 1.475(2) and 1.328(4) Å for **1a** and **1b**, respectively) corresponding to a localized system of C=C–C bonds.

The benzene rings in the stilbene systems of **1a, b** exhibit some bond length redistribution, apparently caused by electronic effects of the alkoxy moieties. The C(5)–C(6) bonds (1.414(2), 1.417(2) Å) are elongated compared to most of the other bonds in the benzene rings. Two angles O(2)–C(6)–C(5) and O(1)–C(5)–C(6), exocyclic with respect to the benzene rings, are reduced (114.9(1)—115.9(1)°), whereas two other angles, O(2)–C(6)–C(7) and O(1)–C(5)–C(4), endocyclic with respect to the benzene rings, are increased (124.9(1)–125.2(2)°).

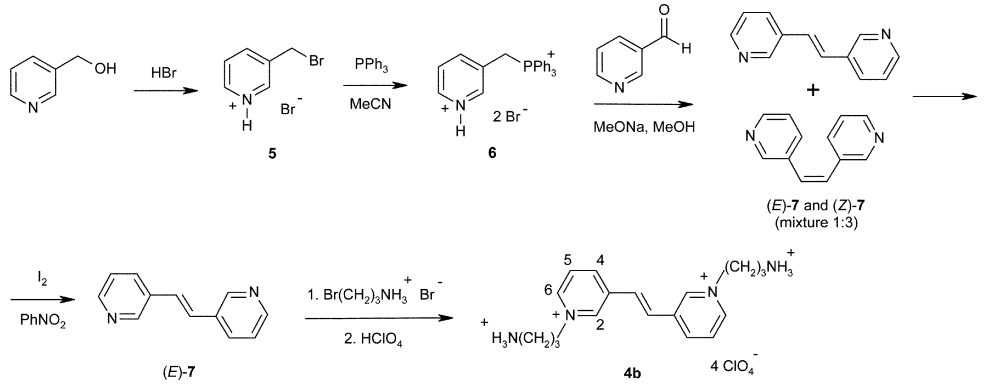

Scheme 3 Synthesis of acceptor **4b**.

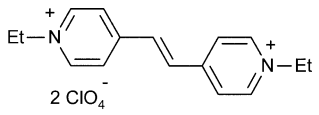

2a

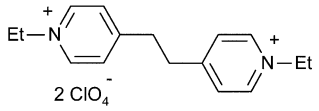

3a

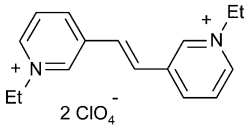

4a

Scheme 4 Model acceptors **2a**, **3a**, and **4a**.

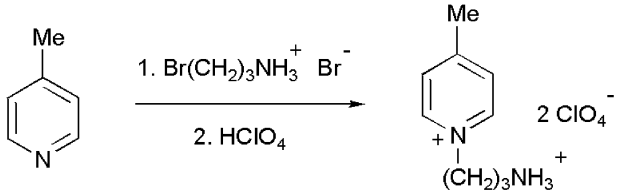

8

Scheme 5 Synthesis of model acceptor **8**.

The O(1)···O(2) distances (2.591(3), 2.591(1) Å) are shortened compared to twice the van der Waals radius (~2.8 Å) of oxygen. Interestingly these distances could be elongated if the exocyclic angles were equal to the standard value (120°). These geometric peculiarities are apparently due to both the steric repulsion of the O(1) and O(2) atoms and the conjugation of the lone electron pairs (LEPs) of these atoms with the π-system of the benzene rings. Both oxygen atoms, O(1) and O(2), have a geometry favourable for this conjugation. Indeed, the bond angles at the O(1) and O(2) atoms in **1a, b** (116.7(1)–117.1(1)°) imply sp^2 hybridization of these atoms, unlike the bond angles at O(3)–O(6) in **1b** (112.1(1)–113.0(2)°), which are typical of the sp^3 hybridization state of these oxygen atoms. The C_{Alk}–O(2)–C(6)–C(5) and C(8)–O(1)–C(5)–C(6) torsion angles (−167.5 and 169.2°, 165.7 and −175.5° for **1a** and **1b**, respectively) are close to the values most suitable for the conjugation of the LEP in the p orbital of each of O(1) and O(2) atoms with the benzene ring π-systems. It should be mentioned that similar geometric features have been observed previously in benzo-18-crown-6 butadienyl[10] and in dithia-18-crown-6 styryl[11] dyes.

In **1b**, the oxygen atoms of the 18-crown-6 subunit form a hexagon in which the shorter diagonals vary within 2.59–2.96 Å. The least-squares mean plane through the oxygen atoms is inclined with respect to the benzene ring plane by 39.7° (see Fig. 1).

Two layers of crystal packing of **1a** are shown in Fig. 2. No stacking packing motif of stilbene molecules from the adjacent layers is observed here. The mutual arrangement of the layers may be attributed to a "staircase" packing motif where adjacent "staircases" are arranged in parallel:

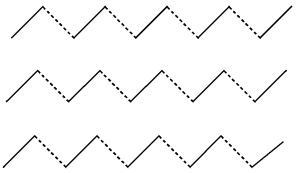

Interestingly the methoxy groups of adjacent molecules tend to form extended hydrophilic areas in the crystal. It is likely that this tendency precludes the formation of a stacking packing motif, which is more typical of conjugated organic compounds than the "staircase" one.

The crystal packing of **1b** is shown in Fig. 3. The molecules are also arranged in the "staircases". The axes of adjacent "staircases" run in parallel along the *b*-axis. However, the staircases are arranged in the herringbone-type packing:

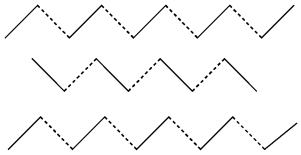

The herringbone-type packing is a crystal packing typical of large conjugated or aromatic molecules.[12] In the crystal, the crown ether fragments form loosely packed double hydrophilic layers (Fig. 3). The formation of loosely packed areas by crown ether subunits is characteristic of the crystal structures of all the crown ether dyes we have investigated previously.

Recently,[9] the X-ray structures of **2a–4a** have also been determined. The structures of the dicationic moieties in these model acceptors are shown in Fig. 4. The dication central fragment has a nearly planar structure in **2a** and **4a** but it is non-planar in **3a**. The ethylene bond lengths are equal to 1.345(4) Å in **2a** and 1.333(7), 1.328(4) Å in **4a**, whereas both neighbouring formally single bonds are equal to 1.465(5), 1.457(5) Å in **2a** and 1.467(4)–1.471(5) Å in **4a**. These bond length distributions suggest stronger π-conjugation between

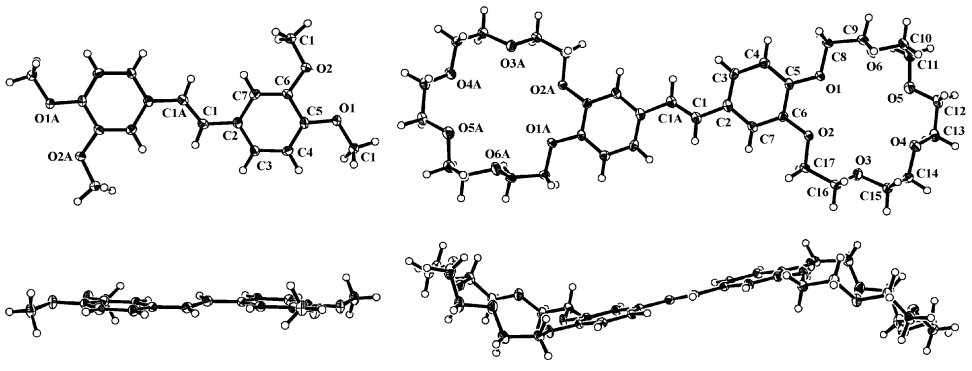

1a **1b**

Fig. 1 Structure of molecules **1a** and **1b** in the frontal and side projections showing 50% probability of thermal anisotropic atom displacement parameters.

Downloaded by University of California - Los Angeles on 01 January 2013
Published on 11 May 2005 on http://pubs.rsc.org | doi:10.1039/B500667H

View Article Online

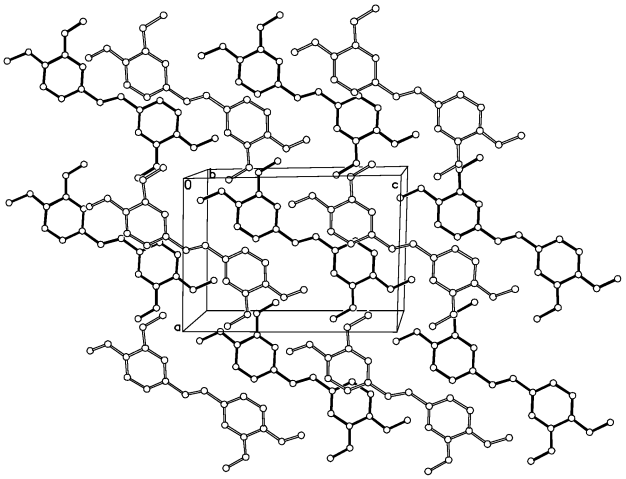

Fig. 2 Two layers of the crystal packing of **1a**.

Downloaded by University of California - Los Angeles on 01 January 2013
Published on 11 May 2005 on http://pubs.rsc.org | doi:10.1039/B500667H

the pyridine rings in **2a** as compared with that in **4a**. The ethyl substituents in **2a–4a** point in opposite directions relative to the mean plane of the unsaturated systems. This denotes that acceptors **2–4** are pre-organized to form 2 : 1 D–A complexes.[9]

C. Absorption and fluorescence studies

The complexation of bis(crown) stilbene **1b** with viologen analogues **2a, b** and various diammonium salts of the alkane series, such as dodecanediammonium diperchlorate (**9**), in acetonitrile has been recently studied by steady-state electronic spectroscopy.[5] Stilbene **1b** was reported to form highly stable 1 : 1 complexes with diammonium compounds **2b** and **9** *via* two-centre host–guest bonding (Scheme 6). The 1 : 1 complex [**1b** · **2b**] shows an increased thermodynamic stability (Table 1), which is attributed to additional through-space interactions leading to charge transfer from π-electron donor **1b** to π-electron acceptor **2b**. The charge-transfer (CT) interactions in [**1b** · **2b**] are evidenced by the presence of a broad CT band (λ_{max} = 502 nm) in the absorption spectrum and total fluorescence quenching.

It was also found that stilbene **1b** can react with the complex [**1b** · **2b**] to produce the termolecular CT complex [(**1b**)$_2$ · **2b**] (Scheme 6). The latter is supposed to have a sandwich-type layered structure in which the acceptor **2b** is located between two complexed molecules of the biscrown stilbene.

Hereinafter the thermodynamic stability of bi- and termolecular D–A complexes is discussed in terms of the corresponding formation constants K_1 and K_2 associated with the following equilibria

$$D + A \overset{K_1}{\rightleftarrows} DA \qquad (1)$$

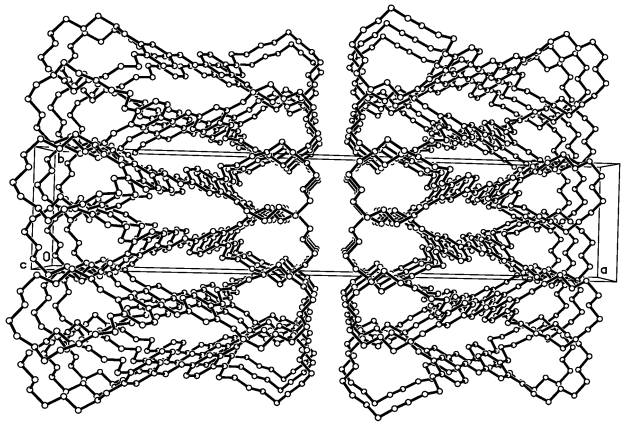

Fig. 3 Crystal packing of molecules **1b**.

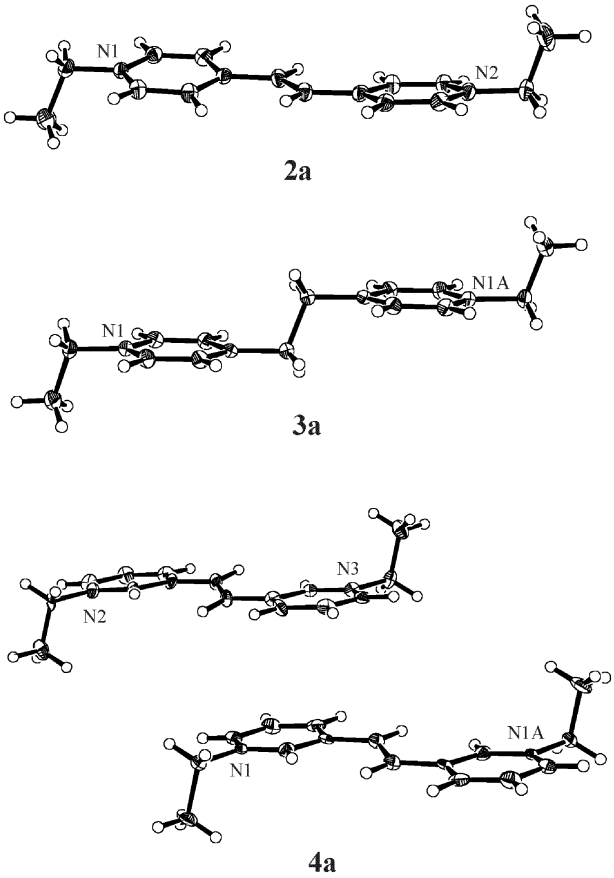

Fig. 4 Structures of the cations in **2a–4a** (two independent molecules for **4a**) showing 50% probability of thermal anisotropic atom displacement parameters.

and

$$DA + D \overset{K_2}{\rightleftarrows} D_2A \qquad (2)$$

or

$$DA + A \overset{K_2}{\rightleftarrows} DA_2, \qquad (3)$$

where K_1 = [DA]/([D][A]) is the formation constant for a bimolecular D–A complex and K_2 is the formation constant for a termolecular D–A complex (for 2 : 1 D–A complexes, K_2 = [D_2A]/([DA][D]), and for 1 : 2 D–A complexes, K_2 = [DA_2]/([DA][A]).

The log K_2 value for [(**1b**)$_2$ · **2b**] was estimated to be 3.20,[5b] which corresponds to a Gibbs free energy ($-\Delta G$) of about 4.3 kcal mol^{-1}. This is much higher than the Gibbs free energy expected for purely CT interactions, $-\Delta G$ < 1.5 kcal mol^{-1}, which was estimated from the log K_1 value for the 1 : 1 complexation between **1b** and the reference acceptor **2a**. Since the numbers of intermolecular N–H···O bonds in complexes [**1b** · **2b**] and [(**1b**)$_2$ · **2b**] are the same, the question arises of what the driving force of the reaction giving [(**1b**)$_2$ · **2b**] is. The following hypothesis has been proposed.[5b] Effective two-centre host–guest bonding between a ditopic receptor and a diammonium dication requires geometric correspondence of these molecules. In the case of **1b** and **2b**, this correspondence appears far from being perfect and, therefore, complex [**1b** · **2b**] is substantially sterically strained. The strain energy can be released in the reaction giving complex [(**1b**)$_2$ · **2b**] (eqn. (2)), thus making a considerable contribution to the reaction ΔG value.

In order to test this hypothesis, we performed a comparative study of the complexation of **1b** with acceptors **2c**, **3b**, and **4b**, which differ from **2b** in geometric features or in π-acceptor

View Article Online

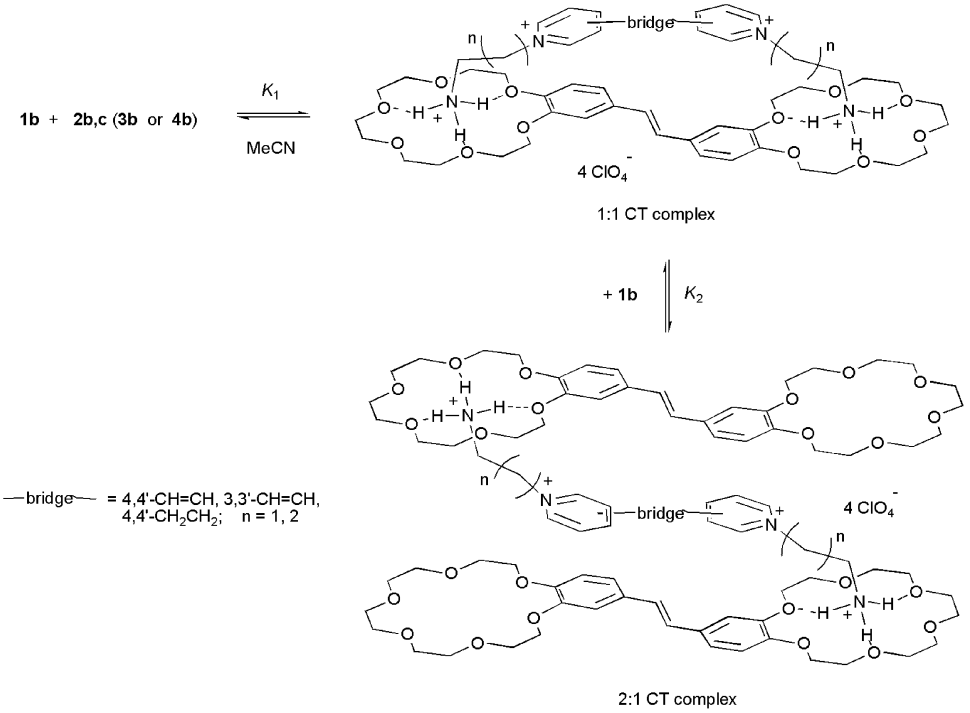

Scheme 6 Complex formation between donor **1b** and diammonium acceptors **2–4**.

Downloaded by University of California - Los Angeles on 01 January 2013
Published on 11 May 2005 on http://pubs.rsc.org | doi:10.1039/B500667H

strength. Figs. 5 and 6 show the CT absorption spectra of the 1 : 1 and 2 : 1 complexes of **1b** with **2b–4b** and **2c** in acetonitrile measured over the 400–700 nm range. The main characteristics of the CT absorption bands are given in Table 1. Note that the uncomplexed compounds do not reveal any absorption within the given spectral range.

According to Mulliken's theory, the formation of a D–A complex involves the interaction between the HOMO of the donor and the LUMO of the acceptor. The π-acceptors **2b** and **2c** have closely similar structures suggesting nearly equal LUMO energies. However, the lowest-energy CT absorption band of [**1b** · **2c**] is shifted bathochromically relative to that of [**1b** · **2b**], which indicates stronger CT interaction between the donor and the acceptor in [**1b** · **2c**]. This effect presumably arises from the shorter donor–acceptor separation distance in [**1b** · **2c**]. In contrast, the lowest-energy CT absorption band of [**1b** · **4b**] is strongly shifted to the blue region and reveals itself as a long-wavelength shoulder of the higher-energy CT band. This shift is attributable to the fact that acceptor **4b** has a higher LUMO energy owing to relatively weak π-conjugation between the β-substituted pyridine rings (see also the characteristics of model acceptors **2a** and **4a** in the X-ray diffraction section). With [**1b** · **3b**], the hypsochromic shift of the lowest-energy CT band is even greater because of the total disruption of the π-conjugation between the pyridine rings in **3b**.

The termolecular complexes [(**1b**)$_2$ · **2b**], [(**1b**)$_2$ · **2c**], [(**1b**)$_2$ · **3b**], and [(**1b**)$_2$ · **4b**] exhibit more intense CT absorption in comparison with the corresponding bimolecular complexes. The clear-cut CT bands of [(**1b**)$_2$ · **2b**] and [(**1b**)$_2$ · **2c**] are shifted bathochromically relative to the corresponding bands of [**1b** · **2b**] and [**1b** · **2c**]. We suppose that the main factors responsible for this shift are as follows. First, the supramolecular D–A–D complexes in comparison with the related D–A dyads likely have less sterically strained structures permitting shorter donor–acceptor separation distances. Second, the termolecular complexes in comparison with the related D–A dyads may have a slightly reduced oxidation potential of the donor because one of the two crown ether fragments in each donor component of the D–A–D triad is free of ammonium ion (Scheme 6).

The formation constants for the bi- and termolecular complexes of **1b** with **2a–c**, **3b**, and **4b** are collected in Table 1. The acceptors with violated π-conjugation between the pyridine

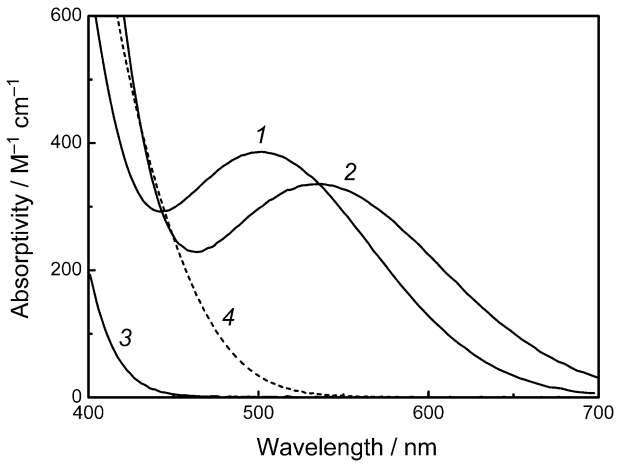

Fig. 5 CT absorption spectra of [**1b** · **2b**] (1), [**1b** · **2c**] (2), [**1b** · **3b**] (3), and [**1b** · **4b**] (4) in MeCN.

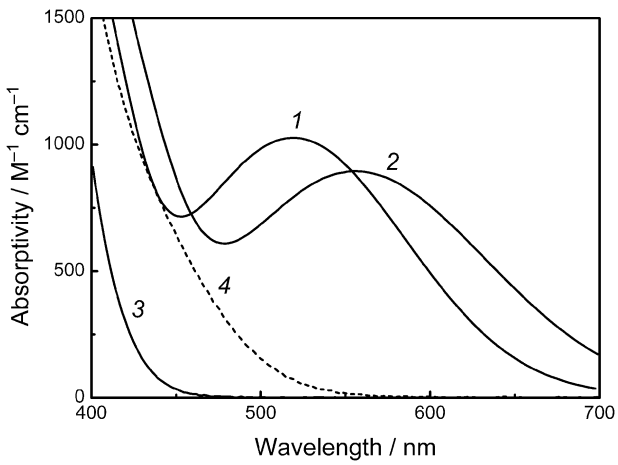

Fig. 6 CT absorption spectra of [(**1b**)$_2$ · **2b**] (1), [(**1b**)$_2$ · **2c**] (2), [(**1b**)$_2$ · **3b**] (3), and [(**1b**)$_2$ · **4b**] (4) in MeCN.

View Article Online

Table 1 Formation constants and UV/Vis absorption data for complexes of stilbenes **1a**, **b** with the π-acceptors **2a–c**, **3a**, **b**, **4a**, **b**, and the model compounds **8** and **9**

Complex	Log K_1 (log K_2)[a]		λ_{max}/nm[b]	ε_{max}/M^{-1} cm^{-1}
	From UV/Vis titration[c]	From ^{1}H NMR titration[d]		
Free **1b**			336	37 500
[**1b** · **9**]	8.59[e]		333.5	38 700
[**1b** · **8**]		4.64	<400	
[**1b** · (**8**)$_2$]		(2.91)	<400	
[**1b** · **2b**]	9.08[e]		502	390
[**1b** · **2c**]	9.42		535	340
[**1b** · **3b**]	8.66		<400	
[**1b** · **4b**]	8.67		405[f]	430[f]
[(**1b**)$_2$ · **2b**]	(3.20)[e]	(3.27)	519	1020
[(**1b**)$_2$ · **2c**]	(2.73)	(2.78)	555	900
[(**1b**)$_2$ · **3b**]	(2.54)	(2.56)	<400	
[(**1b**)$_2$ · **4b**]	(2.18)	(2.02)	416[f]	790[f]
[**1b** · **2a**]	1.13[e]	1.14	527	570
[**1b** · **3a**]		<0.5[g]	<400	
[**1b** · **4a**]		0.99		
[**1a** · **2a**]		~0.5[g]		
[**1a** · **2b**]		~0.5[g]		

[a] K_1 = [DA]/([D][A]) is the formation constant for a 1 : 1 D–A complex; K_2 is the formation constant for a termolecular complex (for 2 : 1 D–A complexes, K_2 = [D_2A]/([DA][D]), and for 1 : 2 D–A complexes, K_2 = [DA_2]/([DA][A]); the formation constants are measured to within about ±20%. [b] Peak position of the lowest-energy absorption band. [c] Anhydrous MeCN, 22 ± 2 °C. [d] MeCN-d_3, 25 ± 1 °C. [e] From ref. 5*b*. [f] Estimated using LogNormal deconvolution. [g] Estimated by postulating the values of $\Delta\delta_H = \delta_H$(complex) − δ_H (single component).

rings, *i.e.* **3b** and **4b**, form less stable bi- and termolecular complexes with stilbene **1b** than compounds **2b, c**. The main reason for this is, apparently, weaker CT interactions in complexes involving **3b** and **4b**. The complex [**1b** · **2c**] shows a higher stability with respect to complex [**1b** · **2b**]; however, the log K_2 value with **2c** is almost three times as low as that with **2b**. Both these findings can be explained by the fact that complex [**1b** · **2c**] is formed with lower steric strain than [**1b** · **2b**] owing to more exact geometric matching between **2c** and **1b** for the two-centre host–guest bonding. According to the above hypothesis, a reduction of the steric strain in the bimolecular complex should not only increase the thermodynamic stability of this complex, but also decrease the log K_2 value.

Previously, we reported that the supramolecular complex [**1b** · **2b**] can act as a fluorescent sensor for metal ions.[5a] Taking the [**1b** · **2b**] + $Ba(ClO_4)_2$ system as an example, we have shown that metal ions can displace the diammonium salt in a non-fluorescent CT complex, which gives rise to substantial fluorescence from metal complexed bis(crown) stilbene‡ (Scheme 7).

In order to evaluate the selectivity of the fluorescence response, we carried out a comparative study of the emission behaviour of acetonitrile solutions of [**1b** · **2b**] in the presence of $Mg(ClO_4)_2$, $Ca(ClO_4)_2$, and $Ba(ClO_4)_2$. The results are presented in Fig. 7. A dilute solution of [**1b** · **2b**] (2×10^{-6} M) shows a very weak fluorescence, which is due to the fact that a small fraction of molecules **1b** and **2b** occur in the free state. The optical properties of this solution barely change upon the addition of $Mg(ClO_4)_2$ up to a five-fold excess with respect to the D–A complex. However, the addition of small amounts of $Ca(ClO_4)_2$, or $Ba(ClO_4)_2$ induces a substantial fluorescence

‡ The fluorescence quantum yield of free **1b** in acetonitrile is about 0.3.[5a] Upon the complexation of **1b** with $Ba(ClO_4)_2$, the fluorescence quantum yield increases by ~10%.

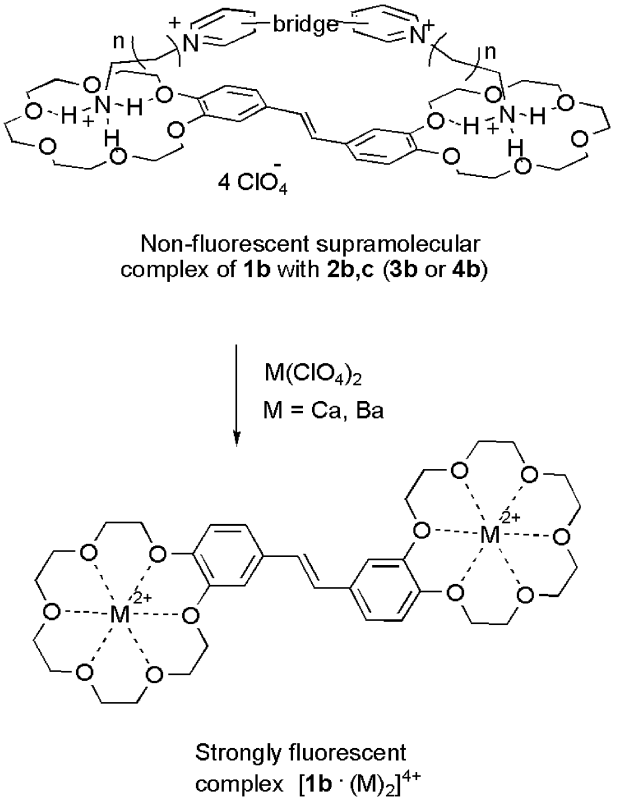

Scheme 7 Reactions of CT complexes with metal salts.

enhancement. The quantitative analysis of the dependences shown in Fig. 7 is complicated by the fact that **1b** can form metal complexes of different compositions (1 : 1 and 1 : 2), which can show different fluorescent properties. However, the patterns of these dependences imply that the ability of **1b** to bind Ba^{2+} and Ca^{2+} ions is much higher than its ability to bind tetracation **2b**. This may be a reason for low selectivity of the fluorescence response of this system to Ba^{2+} compared to Ca^{2+}.

D. ^{1}H NMR spectroscopy studies

According to X-ray diffraction (Fig. 1), tetramethoxystilbene (*E*)-**1a** and bis(18-crown-6)stilbene (*E*)-**1b** exist in the crystalline state as symmetric *syn*,*syn*- and *anti*,*anti*-conformers, respectively, which is probably due to the closest packing of molecules requirements. In CD_3CN solutions, the *anti*,*anti*-,

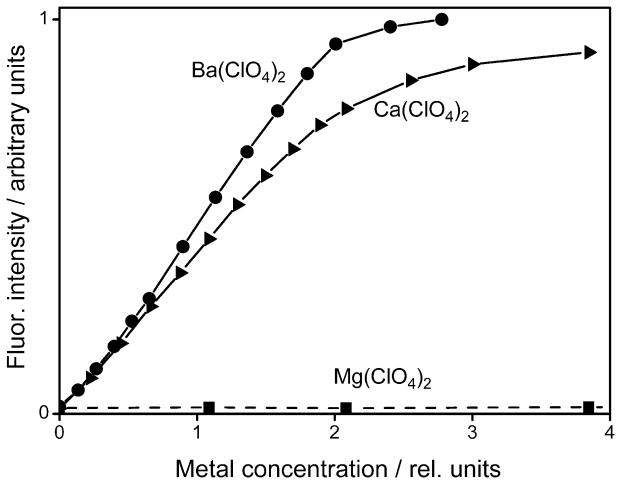

Fig. 7 Fluorescence from an acetonitrile solution of [**1b** · **2b**] (2×10^{-6} M) as a function of the relative concentration of metal perchlorate added. The observation wavelength is 375 nm.

Downloaded by University of California - Los Angeles on 01 January 2013
Published on 11 May 2005 on http://pubs.rsc.org | doi:10.1039/B500667H

View Article Online

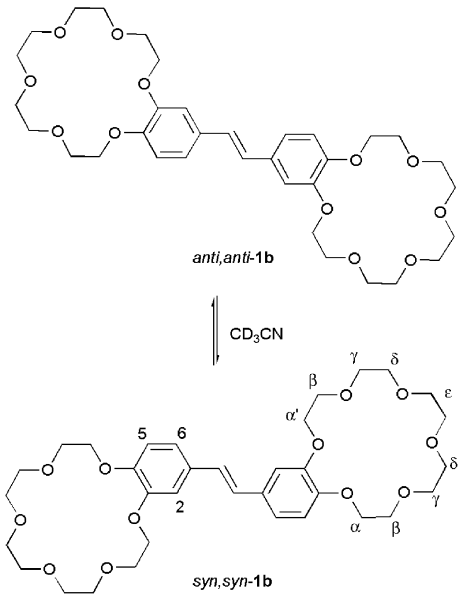

Scheme 8 Conformers of (*E*)-**1b**.

anti,*syn*-, and *syn*,*syn*-conformers of **1a**, **b** may coexist (Scheme 8), by analogy with the crown-containing styryl and butadienyl dyes.[10,13] Unfortunately, the NOE spectra do not provide the possibility of estimating the equilibrium content of both symmetric conformers of **1a**, **b** due to substantial interaction of the ethylene bond protons with both the H-2 and H-6 protons (see atom numbering in Scheme 8). However, in view of the fact that the signals for H-2 in the ^{1}H NMR spectra are shifted downfield relative to the H-6 signals, one can suggest that the more compact *syn*,*syn*-form, in which H-2 falls in the deshielding region of the ethylene bond, predominates (see also the ^{13}C NMR section). The chemical shifts for the crown ether aliphatic protons of **1b** are ordered as follows: the longer the distance between the observed proton and the benzene ring, the smaller the proton chemical shift. According to the NOE spectrum, the proton signals for the α′-CH_2O groups are shifted downfield relative to those for the α-CH_2O groups. Apparently, the protons of α′-CH_2O experience the deshielding influence of the ethylene bond, like the H-2 aromatic protons.

Fig. 8 shows the changes in the proton chemical shifts induced by complexation, $\Delta\delta_H = \delta_H$(complex) − δ_H(single component), for stilbene **1b** and the diammonium salts **9**, **2b**–**4b**, and **2c** in CD_3CN. The $\Delta\delta_H$ values were measured for equimolar D–A mixtures with a concentration of about 1×10^{-3} M. The NMR titration showed that the reactants exist almost entirely as 1 : 1 complexes under these conditions. For comparison, Fig. 8 shows the changes in the proton chemical shifts that accompany the complexation of **1b** with two ethylammonium ions. Complex $[\mathbf{1b}\cdot(EtNH_3)_2]^{2+}$ was prepared by addition of a large excess ($\sim 2 \times 10^{-2}$ M) of ethylammonium perchlorate to a CD_3CN solution of **1b** (2×10^{-3} M).

The interaction of the crown ether fragments of **1b** with the $EtNH_3^+$ ions in $[\mathbf{1b}\cdot(EtNH_3)_2]^{2+}$ through N–H···O hydrogen bonds brings about downfield shifts of all the proton signals of bis(crown) stilbene ($\Delta\delta_H$ = 0.07–0.13 ppm). One could expect that the complexation would shift the conformational equilibrium for **1b** to the more extended *anti*,*anti*-conformer in which the Coulomb interaction between the complexed ammonium ions is lower. However, this apparently does not take place, because the distance between the H-2 and H-6 proton signals (0.12 ppm) barely changes upon complexation.

Comparison of the $\Delta\delta_H$ values for complexes $[\mathbf{1b}\cdot(EtNH_3)_2]^{2+}$ and $[\mathbf{1b}\cdot\mathbf{9}]$ shows that the polymethylene bridge that links the two ammonium ions in complex $[\mathbf{1b}\cdot\mathbf{9}]$ does not influence significantly the positions of the proton signals for complexed bis(crown) stilbene. The signals of all the methylene protons of **9** shift upfield upon complexation. For the protons located near the NH_3^+ groups, this effect is not very pronounced ($\Delta\delta_H = -0.18$ ppm) and can be rather attributed to a decrease in the charge on the ammonium group due to its delocalization over the crown ether oxygen atoms. The substantial shifts of the signals of other methylene protons of **9** ($\Delta\delta_H$ up to −0.58 ppm) are due to the shielding effect from the system of conjugated π-bonds of **1b** above which the methylene bridge is located.

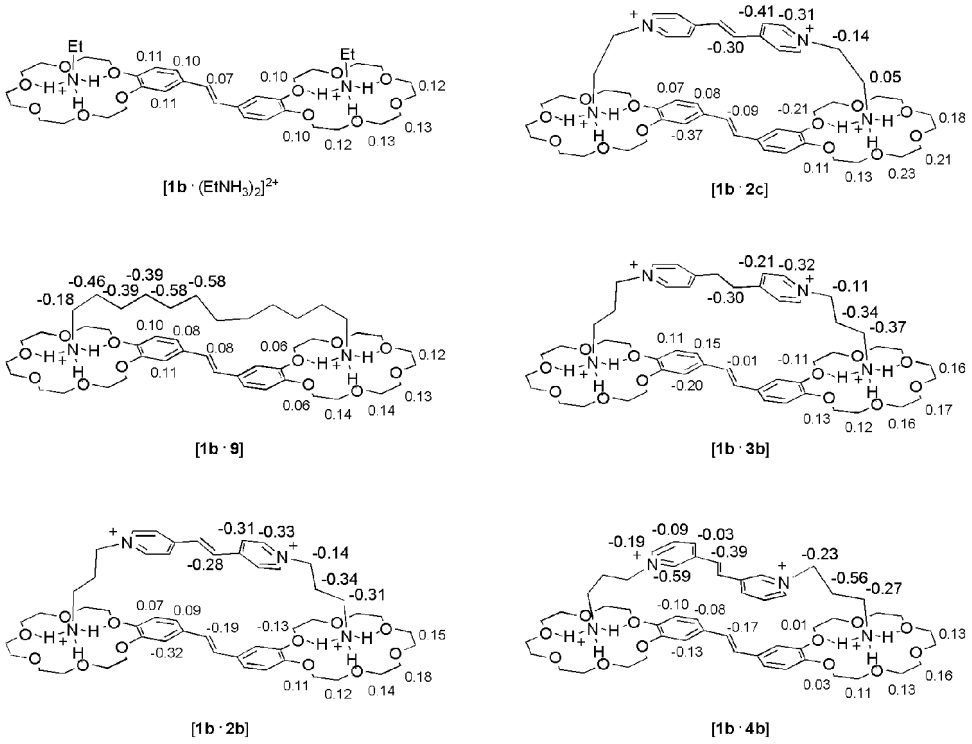

Fig. 8 Changes in the proton chemical shifts, $\Delta\delta_H = \delta_H$(complex) − δ_H(single component), upon complexation of **1b** with $EtNH_3^+ClO_4^-$, **9**, **2b**–**4b**, and **2c** in CD_3CN at 25 °C.

Downloaded by University of California - Los Angeles on 01 January 2013
Published on 11 May 2005 on http://pubs.rsc.org | doi:10.1039/B500667H

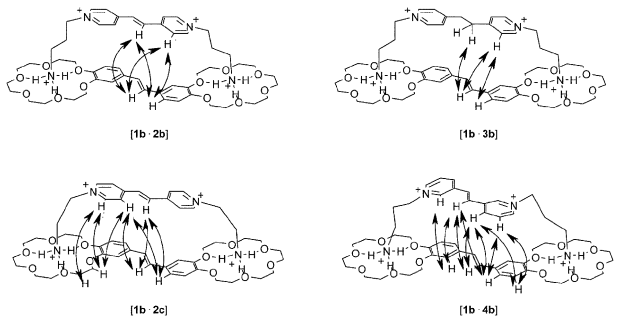

Fig. 9 Intermolecular NOE interactions detected for the supramolecular D–A complexes.

As expected, the coordination of the terminal ammonium groups of the π-acceptor to the crown ether fragments of the π-donor in supramolecular D–A complexes [**1b** · **2b**], [**1b** · **2c**], [**1b** · **3b**], and [**1b** · **4b**], induces a downfield shift (up to 0.23 ppm) of the signals for most of the CH_2O groups. In contrast to the complex [**1b** · **9**], the D–A dyads show negative $\Delta\delta_H$ values for some protons of the stilbene fragment. Pronounced upfield shifts are also observed for the signals of the central fragment of the π-acceptors. These effects are due to the mutual shielding of the systems of conjugated π-bonds in the donor and acceptor components of the complex.

Fig. 9 shows the NOE interactions detected for [**1b** · **2b**], [**1b** · **2c**], [**1b** · **3b**], and [**1b** · **4b**]. All intermolecular NOE cross-peaks had low intensities compared to the intramolecular peaks. This is indicative of relatively long distances (3.5–5 Å) between the interacting protons of the donor and the acceptor in the D–A complexes.

The fact that the intermolecular (through-space) interactions between the donor and the acceptor in the supramolecular D–A complexes are clearly seen in the ^{1}H NMR spectra can be used to determine the mutual spatial arrangement of the complex components. The D–A complexes involving acceptors with identical topologies, *i.e.* [**1b** · **2b**], [**1b** · **2c**] and [**1b** · **3b**], show similar distributions of the $\Delta\delta_H$ values (Fig. 8) and similar intermolecular NOE interactions (Fig. 9), suggesting a similar relative orientation of the donor and acceptor components. In these dyads, just a few protons of **1b** (H-2, and the protons of the ethylene bond and the α′-CH_2O groups) experience significant shielding effects of the unsaturated fragments of the acceptor. This implies that the one-plane projections of the π-donor and π-acceptor moieties in these complexes overlap preferably according to the X-pattern rather than lie strictly above each other. With this geometry, the H-2 and H-6 protons of the pyridine rings (numbering in Scheme 2) should fall to different extents into the shielding regions of **1b**; however, these protons show the common narrow signal, which is attributable to exchange processes that are fast on the ^{1}H NMR time scale, in the D–A dyads. The same exchange processes also affects the H-3 and H-5 protons of the pyridine rings.

Acceptor **4b** differs from **2b, c** and **3b** in topology. The presence of 1,3-disubstituted pyridine rings implies that **4b** can adopt different *s*-conformations by analogy with **1b**. Complex [**1b** · **4b**] shows a specific distribution of $\Delta\delta_H$ values, in particular, all aromatic protons of **1b** in this complex are characterized by negative $\Delta\delta_H$ values becoming closer together. The number of intermolecular NOE interactions found for [**1b** · **4b**] is the greatest among the D–A complexes studied. These observations seem to imply a greater overlap of the one-plane projections of the π-donor and π-acceptor moieties in complex [**1b** · **4b**].

As noted in the previous Section, the interactions determining the thermodynamic stability of supramolecular D–A complexes can be conventionally classified into two types, namely, relatively strong two-centre host–guest interactions and much weaker through-space interactions between the donor and acceptor π-systems, resulting in charge transfer. In order to estimate the possible contribution of the through-space interactions to the Gibbs free energy of complex formation, we studied several model systems, **1a**/**2a**, **b** and **1b**/**2a**–**4a**, by ^{1}H NMR titration.

The formation of weak 1 : 1 D–A complexes was observed for all model systems. The log K_1 values for [**1b** · **2a**] and [**1b** · **4a**] and the changes in the proton chemical shifts upon complete complexation, $\Delta\delta_H$, for **2a** and **4a** were calculated from the titration curves using the HYPNMR program.[14] For other model systems, the degree of complex formation was too low for exact extrapolation of the titration curves; therefore, the log K_1 values were estimated by postulating the value $\Delta\delta_H = -0.60$ ppm for the protons of the central group of the π-acceptor. The log K_1 values are listed in Table 1, and the $\Delta\delta_H$ values for **2a–4a** are shown in Fig. 10.

For acceptors **2a–4a**, the $\Delta\delta_H$ values tend to decrease as the distance from the centre of the molecule increases, whereas for the corresponding diammonium compounds **2b–4b**, this tendency is not observed (Fig. 8). This indicates that the relative orientation of the donor and the acceptor in model D–A systems shows a more clear-cut X-pattern than that in supramolecular D–A complexes based on diammonium compounds. This comes as no surprise, because the geometry of the supramolecular D–A complexes is mainly determined by the two-centre host–guest interaction, which accounts for a relative orientation of the donor and acceptor moieties other than that favourable for the through-space interaction.

The tetramethoxystilbene complexes, [**1a** · **2a**] and [**1a** · **2b**], have lower log K_1 values than [**1b** · **2a**], despite the fact that the oxidation potentials of stilbenes **1a** and **1b** are equal.[15] Presumably, in addition to the weak CT interactions between the π-systems of **1b** and **2a**, weak interactions of the electrostatic nature between the crown ether oxygen atoms of **1b** and the positively charged ethylpyridinium fragments of **2a** occur in the [**1b** · **2a**] complex.

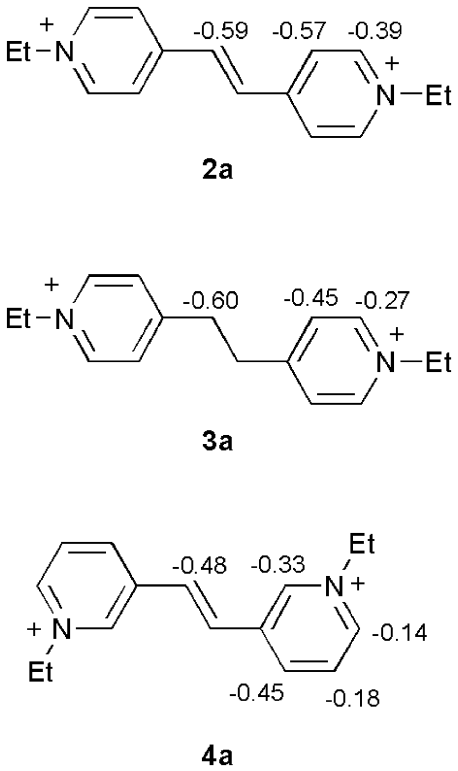

Fig. 10 Changes in the proton chemical shifts, $\Delta\delta_H = \delta_H$(complexed form) − δ_H(free form), upon 1 : 1 complexation of **2a–4a** with **1b**.

Downloaded by University of California - Los Angeles on 01 January 2013
Published on 11 May 2005 on http://pubs.rsc.org | doi:10.1039/B500667H

View Article Online

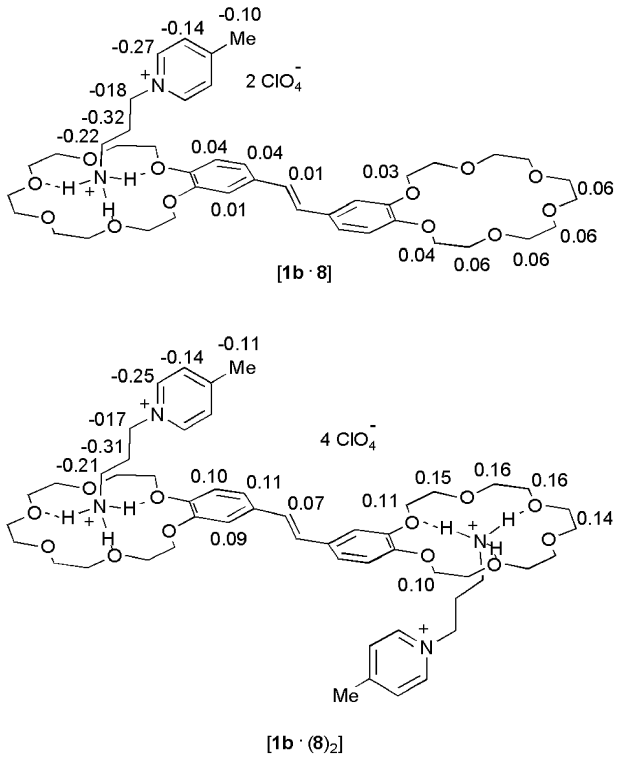

Fig. 11 Changes in the proton chemical shifts, $\Delta\delta_H = \delta_H$(complex) − δ_H(single component), upon 1 : 1 and 1 : 2 complexation between **1b** and **8**.

We studied yet another model system incorporating bis(crown) stilbene **1b** and the ammonium derivative of 4-methylpyridine **8**. The ^{1}H NMR titration data for this system complied well with the reaction model that includes two equilibria (eqn. (1) and eqn. (3)) and implies the formation of complexes [**1b** · **8**] and [**1b** · (**8**)$_2$]. The log K_1 and log K_2 values for these complexes are given in Table 1.

The doubled log K_1 value for the one-centre complex [**1b** · **8**] (2 log K_1 = 9.28) is substantially greater than the value log K_1 = 8.66 for the related two-centre complex [**1b** · **3b**]. This fact is in line with the hypothesis about substantial steric strain in supramolecular D–A complexes of type [**1b** · **3b**] or, at least, does not contradict this hypothesis. The equilibrium constant K_2 for the association of **8** and [**1b** · **8**] (eqn. (3)) is substantially lower than the formation constant K_1 for complex [**1b** · **8**] due to the Coulomb repulsion between two cations **8**.

Fig. 11 shows the values $\Delta\delta_H = \delta_H$(complex) − δ_H(single component) for [**1b** · **8**] and [**1b** · (**8**)$_2$] calculated from the titration curves. These complexes, like complex [**1b** · $(EtNH_3)_2]^{2+}$, are characterized by downfield shifts of all proton signals of bis(crown) stilbene. All the proton signals of the acceptor in complexes [**1b** · **8**] and [**1b** · (**8**)$_2$] shift upfield, the $\Delta\delta_H$ values for **8** being virtually independent of the composition of the complex and being close to the $\Delta\delta_H$ values for like protons in complexes [**1b** · **2b**] and [**1b** · **3b**]. These facts indicate that in complexes [**1b** · **8**] and [**1b** · (**8**)$_2$], the acceptor protons fall in the shielding region of the stilbene π-system, but not *vice versa*. This situation arises when the pyridine ring of **8** is situated above the stilbene fragment of **1b** and their planes are perpendicular to each other. Apparently, among the additional through-space interactions, contacts of the CH···π-system type predominate in complexes of **8**, resulting in the cross arrangement of the unsaturated fragments of the donor and the acceptor. The foregoing suggests that in supramolecular complexes with two-centre binding, the diammonium compounds **2b, c**, **3b**, and **4b** can have a twisted geometry of the central fragment, resulting in the accumulation of steric strain, mentioned in the previous Section.

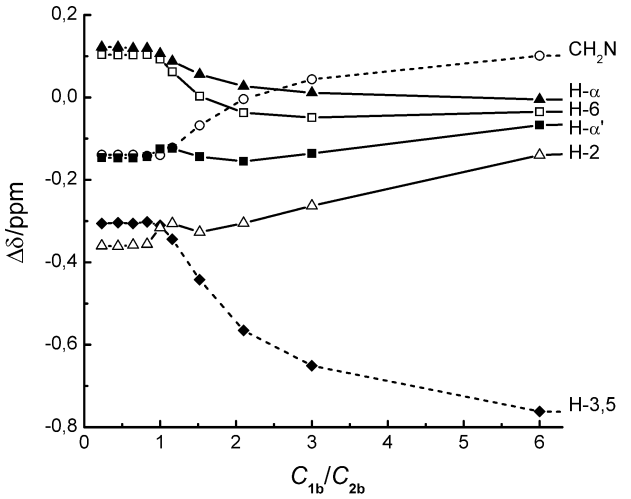

Fig. 12 Values of $\Delta\delta_H = \delta_H$(D/A mixture) − δ_H(single component) for some protons of **2b** (dashed curves) and **1b** (solid curves) in CD_3CN as a function of the donor/acceptor concentration ratio.

According to UV/Vis spectroscopy data, bis(crown) stilbene **1b** and diammonium π-acceptor salts **2c** and **2b–4b** can form not only highly stable D–A complexes but also D–A–D triads (Scheme 6). Additional evidence for the formation of the termolecular complexes was obtained by ^{1}H NMR titration.

Fig. 12 shows the values $\Delta\delta_H = \delta_H$(D/A mixture) − δ_H(single component) for some protons of donor **1b** and acceptor **2b** as a function of the donor/acceptor concentration ratio (C_D/C_A). When $C_D < C_A$, the ^{1}H NMR spectra of the D/A mixtures consisted of two sets of signals, one due to the free form of **2b** and the other, to complex [**1b** · **2b**]. The proton signals for the free and complexed forms of the acceptor were substantially broadened due to exchange between these forms, slow on the ^{1}H NMR time scale. The low rate of the exchange processes accounts for the fact that the $\Delta\delta_H$ values that refer to the protons of the complexed donor and acceptor in Fig. 12 are virtually independent of C_D/C_A when $C_D < C_A$.

The growth of the C_D/C_A ratio in the $C_D > C_A$ region entails a monotonic change in the $\Delta\delta_H$ value for the acceptor protons. The titration curves for the donor protons follow a more complex pattern. These observations are in good agreement with the reaction model discussed above (eqns. (1) and (2)), which implies the formation of a termolecular complex [(**1b**)$_2$ · **2b**]. When $C_D > C_A$, the concentration of the free acceptor is negligibly low, the monotonic variation of $\Delta\delta_H$ for the protons of **2b** being due to the shift of the complexation equilibrium from [**1b** · **2b**] to [(**1b**)$_2$ · **2b**]. The more complex pattern of the variation of $\Delta\delta_H$ with C_D/C_A for the protons of **1b** is due to the fact that the donor can exist as three forms, in particular, as the free molecule and as either of two complexes, [**1b** · **2b**] and [(**1b**)$_2$ · **2b**], with different ratios of the *syn,syn*- to the *anti,anti*-conformers for each form. The lack of separate sets of signals for different forms of the donor or the acceptor at $C_D > C_A$ is due to fast exchange processes caused by relatively low stability of [(**1b**)$_2$ · **2b**].

The dependences of $\Delta\delta_H$ on C_D/C_A for the protons of **2b** in the $C_D > C_A$ region were in good agreement with the simplified reaction model that includes only one equilibrium (eqn. (2)), which made it possible to determine the equilibrium constant K_2 and the chemical shifts for the acceptor protons in complex [(**1b**)$_2$ · **2b**]. The simplified model is applicable to this system due to the large formation constant K_1 for complex [**1b** · **2b**].

For the systems **1b/2c**, **1b/3b**, and **1b/4b**, the results of titration were qualitatively similar to the results obtained for **1b/2b**. The calculated values $\Delta\delta_H = \delta_H$(2 : 1 D–A complex) − δ_H(single component) for the protons of acceptors **2b–4b**

Downloaded by University of California - Los Angeles on 01 January 2013
Published on 11 May 2005 on http://pubs.rsc.org | doi:10.1039/B500667H

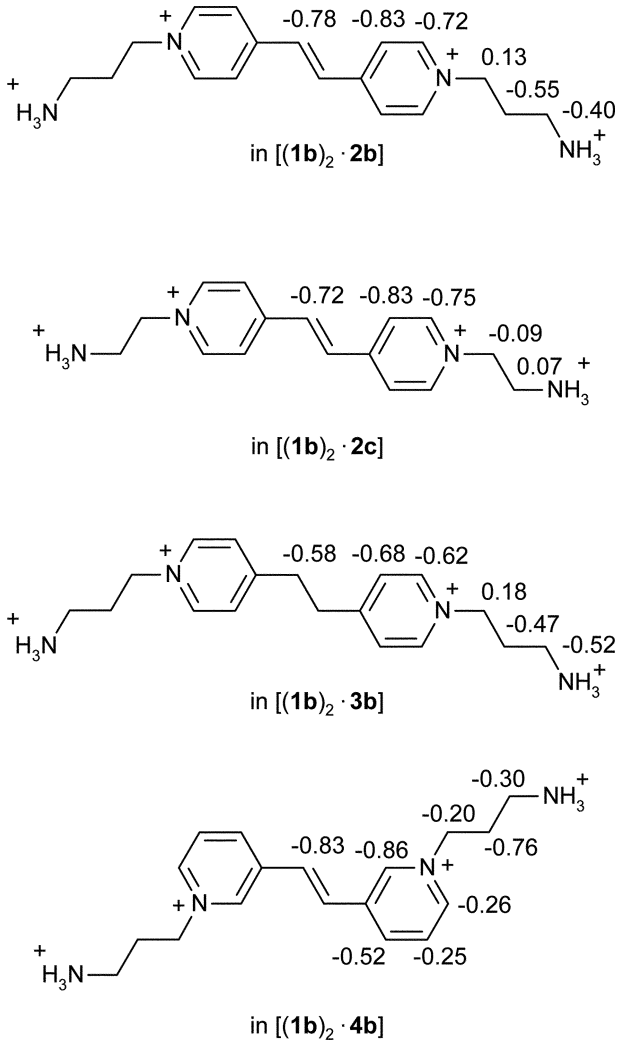

Fig. 13 Changes in the proton chemical shifts, $\Delta\delta_H = \delta_H(2:1\ D–A\ complex) - \delta_H(single\ component)$, for acceptors **2b–4b** and **2c** upon 2 : 1 D–A complexation with donor **1b**.

and **2c** are shown in Fig. 13. The constants K_2 as determined by ^{1}H NMR titration are listed in Table 1.

The results of the NMR study of termolecular D–A complexes are in good agreement with the results of spectrophotometric measurements. For all four systems, **1b/2b–4b** and **1b/2c**, 2(D) : 1(A) complexation induces strong upfield shifts of the proton signals for the central fragment of the π-acceptor, the values of these shifts, $\Delta\delta_H$, being much greater than the corresponding $\Delta\delta_H$ values measured for the related D–A dyads. This observation corroborates the assumptions that termolecular complexes have a sandwich-type layered D–A–D structure and that the donor–acceptor separation distances in these complexes are shorter than those in the related D–A dyads. The shorter distances result from lower steric restrictions for the components of termolecular complexes.

E. ^{13}C NMR spectroscopy studies

Compounds **1b** and **2b** as well as their mixtures were studied using ^{13}C NMR in CD_3CN solutions containing 5% (v/v) of deuterated water. Water was added to increase the solubility of **2b** and its complexes with **1b**. Qualitative ^{1}H NMR experiments have shown that a slight amount of water does not markedly destroy complexes [**1b** · **2b**] and [(**1b**)$_2$ · **2b**]. These observations, together with high working concentrations of compounds (*ca.* 0.02 M) allowed us to infer that in solutions containing 1 : 1 and 2 : 1 mixtures of **1b** and **2b**, the bimolecular and termolecular complexes, respectively, are the major components (> 90%). Some supramolecular complexes were isolated in the solid state (Experimental section). Compounds **1b** and **2b** as well as complex [(**1b**)$_2$ · **2b**] were studied by solid-state ^{13}C NMR. The solution and solid-state ^{13}C NMR data are presented in Table 2S (ESI).†

The solid-state ^{13}C NMR spectrum of **2b** exhibits a set of relatively narrow signals, whose number exceeds the number of lines in the solution ^{13}C NMR spectrum. In solution, the symmetrically arranged carbon atoms of the pyridine rings, C-2 and C-6, and C-3 and C-5, are responsible for averaged signals, one for each pair, owing to fast exchange processes. In the solid state, these signals split. The magnitude of this splitting is greater for the C-3 and C-5 pair, located most closely to the C=C group (5.8 ppm *vs.* 3.0 ppm for the C-2 and C-6 pair). A similar splitting was reported[16] to take place in the solid-state ^{13}C NMR spectra of *E*-azobenzene derivatives. For these compounds, the pair of aromatic carbon atoms closest to the N=N bond is characterized by a greater interval between the signals (12.8–16.9 ppm), the higher-field signal being assigned to the carbon atom toward which the N=N bond points. Similarly, the higher-field signal for the C-3 and C-5 pair in **2b** is assigned to the C-5 atom toward which the C=C bond points (see Scheme 2).

In the solid-state ^{13}C NMR spectrum of **1b**, the number of rather narrow signals in the aromatic region corresponds to the number of sp^2 carbon atoms in this compound and, as follows from X-ray diffraction data, these signals refer to the *anti,anti*-conformer. The signals of C-2, C-5, and C-6 fall within the narrow interval 113.4–114.8 ppm, which complicates their assignment. In the solution ^{13}C NMR spectrum, the signals of C-6 and C-2 are found at 120.0 and 109.7 ppm, respectively, *i.e.*, change to solution induces a significant downfield shift of the C-6 signal (≥ 5.2 ppm) and a significant upfield shift of the C-2 signal (≥ 3.7 ppm); the δ_C values for other sp^2 atoms change by 0.7–2.5 ppm. This behaviour of the C-6 and C-2 signals confirms the existence in solution of a conformer in which the C=C bond points toward the C-2 atom, *i.e.*, the *syn,syn*-conformer of **1b**.

In solution, binding of **1b** with **2b** as a 1 : 1 complex induces slight changes in the carbon chemical shifts for both compounds, which is due to the low sensitivity of the ^{13}C nuclei to anisotropic effects. It is typical, however, that the signals of the sp^2 carbon atoms of **2b** all shift upfield upon complexation (by 0.30–0.81 ppm). Presumably, these one-directional shift changes arise from a slight alteration of the charge on the π-acceptor moiety of **2b** owing to through-space interactions between this moiety and the stilbene fragment of **1b**. Most of the signals for the stilbene sp^2 carbon atoms shift downfield upon complexation (by 0.22–1.10 ppm). Exceptions are provided by the signals of the C-3 and C-4 atoms, which shift upfield by 1.67 and 1.88 ppm, respectively. This irregularity is likely related to the fact that the electronic structure of the stilbene fragment in [**1b** · **2b**] is affected not only by through-space CT interactions but also by two-centre host–guest interaction involving the crown ether oxygen atoms attached to the C-3 and C-4 aromatic atoms of **1b**. The latter interaction may decrease the O–C_{Ar} bond order due to switching of the p-electrons of the O atoms from conjugation with the chromophore system of stilbene to the formation of hydrogen bonds with the complexed NH_3^+ groups. The signals of the crown ether aliphatic carbon atoms do not show any particular trend upon complexation, indicating a conformational dependence of the δ_C values.

In the solution ^{13}C NMR spectrum of [(**1b**)$_2$ · **2b**], all signals for the sp^2 carbon atoms of **2b** are shifted upfield relative to the corresponding signals for the uncomplexed form of **2b**, the magnitudes of these shifts being 2–3 times larger than in the case of [**1b** · **2b**]. This suggests that the total charge transfer to the π-acceptor moiety of **2b** in [(**1b**)$_2$ · **2b**] is larger than that in [**1b** · **2b**]. The signals of the stilbene sp^2 carbon atoms of

Published on 11 May 2005 on http://pubs.rsc.org | doi:10.1039/B500667H
Downloaded by University of California - Los Angeles on 01 January 2013

Downloaded by University of California - Los Angeles on 01 January 2013
Published on 11 May 2005 on http://pubs.rsc.org | doi:10.1039/B500667H

[$(\mathbf{1b})_2 \cdot \mathbf{2b}$] are shifted rather irregularly relative to the corresponding signals for the uncomplexed form of **1b**, *viz*., four signals are shifted downfield, whereas the other three lie in the higher field. It is noteworthy that the signals of the stilbene C-2 atoms for complexes [$(\mathbf{1b})_2 \cdot \mathbf{2b}$] and [$\mathbf{1b} \cdot \mathbf{2b}$] are shifted in the opposite directions relative to the corresponding signal for the uncomplexed form of **1b**. This feature may be related to the fact that one of the two crown ether fragments in each bis(crown) stilbene molecule of [$(\mathbf{1b})_2 \cdot \mathbf{2b}$] is free of ammonium ion, whereas in complex [$\mathbf{1b} \cdot \mathbf{2b}$] both crown ether fragments are complexed.

The solid-state ^{13}C NMR spectrum of the termolecular complex [$(\mathbf{1b})_2 \cdot \mathbf{2b}$] shows a set of highly broadened and, hence, markedly overlapped signals, which hampers their assignment (see ESI†). The observed pronounced broadening of signals due to ^{13}C nuclei shows that no single structure with rigidly fixed arrangement of components exists for [$(\mathbf{1b})_2 \cdot \mathbf{2b}$] in the solid state. This implies insignificant differences between the stabilities of complexes [$(\mathbf{1b})_2 \cdot \mathbf{2b}$] with different conformational compositions and different arrangements of the donor and acceptor components.

Conclusions

Thus, we found that bis(crown) stilbene **1b** and π-acceptors **2–4** containing two ammonioalkyl groups are able to form supramolecular complexes D–A and D–A–D. The stability of complexes is ensured by two types of interaction: (1) rather strong host–guest type complexation between the crown-ether fragments of bis(crown) stilbene and the ammonium groups of the acceptor, and (2) the weak through-space interaction between the donor and acceptor π-systems, resulting in charge transfer. It should be emphasized that owing to numerous hydrogen bonds, the formation of supramolecular charge transfer complexes takes place even in highly dilute solutions (below 10^{-6} M), as opposed to traditional complexes of this type; this allows detailed investigation of charge and electron transfer processes in bimolecular complexes and in trimolecular CT complexes, which are not actually observed in the solutions. The geometry and the π-acceptor ability of the diammonium compounds have a substantial influence on the thermodynamic and spectral properties of these supramolecular CT complexes. The spatial proximity and pre-organization of the donor and acceptor fragments of the components relative to each other in these supramolecular systems allow the formation of CT complexes, in particular, with very weak acceptors. These complexes cannot be detected even at high component concentrations in the case of usual CT complexation in solutions. Highly stable D–A systems based on **1b** and **2–4** can be used as selective fluorescence sensors for metal ions in non-aqueous media.

Experimental

General methods

3,4,3′,4′-Tetramethoxystilbene (**1a**) and bis(18-crown-6)stilbene (**1b**) were prepared according to a published procedure.[7] Compounds **2a–4a** were prepared as described previously.[5a,9] Nicotinaldehyde, 3-pyridylmethanol, triphenylphosphine, 3-bromopropylamine hydrobromide, 2-bromoethylamine hydrobromide, 1,2-di(4-pyridyl)ethylene, 1,2-di(4-pyridyl)ethane, 1,12-dodecanediamine, 4-methylpyridine, and CD_3CN (water <0.05%) were used as received (Merck or Aldrich). $Mg(ClO_4)_2$, $Ca(ClO_4)_2$, and $Ba(ClO_4)_2$ (Aldrich) were dried *in vacuo* at 240 °C.

The melting points measured with a MEL-Temp II apparatus in a capillary are uncorrected.

The solution ^1H and ^{13}C NMR spectra were recorded on Bruker DRX500 and Bruker DRX400 instruments in $CDCl_3$, CD_3CN, DMSO-d_6, or D_2O solutions using the solvent as an internal reference (7.27, 1.96, 2.50, or 4.70 ppm, respectively, for ^1H; 77.00 or 118.10 ppm in $CDCl_3$ or CD_3CN, respectively, for ^{13}C); homonuclear ^1H–^1H COSY and NOESY spectra and heteronuclear ^1H–^{13}C COSY spectra were used to assign the proton and carbon signals. The high-resolution solid-state ^{13}C magic-angle-spinning NMR spectra were recorded on a Bruker AMX500 instrument at 125.77 MHz at ambient temperature using cross-polarization from the protons together with proton decoupling. The rotation speed of the 5 mm zirconium dioxide rotors were 7 kHz. In all cases, the ^{13}C chemical shifts were referenced by replacement against the high-frequency line of solid adamantane at 38.56 ppm.

IR spectra were recorded on a Bruker IFS-113V spectrophotometer in Nujol between KBr plates. Elemental analyses were performed at the microanalytical laboratory of the A. N. Nesmeyanov Institute of Organoelement Compounds in Moscow, Russia. Silica gel (Kieselgel 60, 0.063–0.100 mm, Merck) and aluminium oxide (Aluminiumoxid 90, aktiv neutral, 0.063–0.200 mm, Merck) were used for chromatography. TLC was carried out on DC-Alufolien Aluminiumoxid 60 F_{254} neutral (Typ E) and Kieselgel 60 F_{254} plates (Merck).

Preparations

1,12-Dodecanediammonium diperchlorate (9). This compound was prepared by the addition of an excess of 70% aq. $HClO_4$ to 1,12-dodecanediamine in methanol followed by quantitative precipitation with diethyl ether; white crystals, mp >250 °C (decomp.). IR ν/cm^{-1}: 3247, 3186, 3147 (NH). ^1H NMR (CD_3CN, 25 °C) δ: 1.31 (br s, 16 H, 8 CH_2), 1.62 (m, 4H, 2 $CH_2CH_2NH_3$), 2.94 (t, J = 7.8 Hz, 4H, 2 CH_2NH_3). Anal. calcd. for $C_{12}H_{30}Cl_2N_2O_8$: C, 35.92; H, 7.54; N, 6.98; found: C, 35.85; H, 7.65; N, 6.94%.

3-[(1,1,1-Triphenylphosphonio)methyl]pyridinium dibromide (6). A solution of 3-pyridylmethanol (5.41 g, 0.050 mol) in 64% aq. HBr (53 mL, 0.44 mol) was heated for 5 h at 125 °C and thoroughly evaporated *in vacuo* to give 10.44 g (83%) of 3-(bromomethyl)pyridinium bromide (**5**) as a lacrimatory yellowish solid.[17] Triphenylphosphine (11.87 g, 0.045 mol) was added to a stirred solution of **5** in anhydrous acetonitrile (100 mL). The resulting solution was refluxed for 7 h and cooled, and the precipitate formed was filtered off and washed with 1 : 1 mixture of benzene–CH_2Cl_2 (100 mL) and then with benzene (60 mL) to give 15.18 g of **6** as a white solid. The mother solution was evaporated *in vacuo*, the residue was treated with ethyl acetate, and the insoluble substance was filtered off and washed with ethyl acetate to give an additional 2.79 g of **6** (85% overall yield); mp 273–277 °C. ^1H NMR ($CDCl_3$, 25 °C) δ: 6.33 (d, J = 15.2 Hz, 2H, CH_2P), 7.72 (m, 6H, 3 H-3′, 3 H-5′), 7.86 (m, 9H, 3 H-2′, 3 H-4′, 3 H-6′), 7.93 (br m, 1H, H-5), 8.64 (br s, 1H, H-6), 8.72 (s, 1H, H-2), 8.90 (br d, J = 5.9 Hz, 1H, H-4). Anal. calcd. for $C_{24}H_{22}Br_2NP$: C, 55.95; H, 4.30; N, 2.72; found: C, 55.60; H, 4.32; N, 2.61%.

3-[(*E*)-2-(3-Pyridyl)-1-ethenyl]pyridine [(*E*)-7]. Phosphonium salt **6** (4.80 g, 9 mmol) was added in portions to a stirred solution of sodium (0.54 g, 23 mmol) in methanol (40 mL) at 0 °C under argon. The resulting mixture was stirred for 5 minutes, and a solution of nicotinaldehyde (0.96 mL, 10 mmol) in methanol (12 mL) was added over a period of 20 minutes. The reaction mixture was stirred for 1.5 h at rt and evaporated *in vacuo*. The residue was dissolved in 4% aq. HCl (110 mL) and the solution (pH 1) was extracted with diethyl ether (4 × 50 mL), alkalized with aq. KOH up to pH 14, and extracted with CH_2Cl_2 (4 × 50 mL). The CH_2Cl_2 extracts were evaporated *in vacuo* and the residue (1.21 g) was purified by column chromatography on aluminium oxide using a gradient benzene–ethyl acetate mixture up to 50% of the latter and then a 9 : 1

benzene–ethanol mixture as the eluents. Two fractions were collected. The first contained only the *Z*-isomer (0.47 g) of 3-[2-(3-pyridyl)-1-ethenyl]pyridine [(*Z*)-**7**] as a yellowish oil.[8b] ^{1}H NMR ($CDCl_3$, 25 °C) δ: 6.71 (s, 2H, CH=CH), 7.17 (d d, $J = 7.9$ Hz, $J = 4.8$ Hz, 2H, 2H-5), 7.49 (d t, $J = 7.9$ Hz, $J = 1.6$ Hz, 2H, 2H-4), 8.46 (d d, $J = 4.8$ Hz, $J = 1.5$ Hz, 2H, H-6), 8.48 (d, $J = 1.6$ Hz, 2H, 2H-2). The second fraction was a *ca.* 1 : 1 mixture (0.40 g; overall yield is 51%) of *E*- and *Z*-isomers of the title compound.

A solution of the 1 : 1 mixture of *E*- and *Z*-isomers of **7** (0.40 g, 2.2 mmol) and some crystals of I_2 in nitrobenzene (4 mL) were refluxed for 1 h, cooled to rt, diluted with benzene (15 mL), and extracted with 10% aq. HCl (3 × 25 mL). The aqueous extracts were washed with benzene (4 × 50 mL), alkalized by 10% aq. NaOH to pH 14, and extracted with benzene (4 × 50 mL). The benzene extracts were evaporated *in vacuo* and the residue (0.36 g) was extracted with boiling *n*-heptane (4 × 25 mL). The heptane extracts were evaporated *in vacuo* to give 0.31 g (78%) of (*E*)-**7** as a slightly yellowish solid, mp 87–89 °C. Lit. data for (*E*)-**7**: colourless solid, mp 90 °C.[8b]

Synthesis of *N*,*N*′-di(ammonioalkyl) derivatives of viologen analogues 2b, c, 3b, 4b (general procedure)

Method (a). A mixture of (*E*)-1,2-di(4-pyridyl)ethylene, (*E*)-1,2-di(3-pyridyl)ethylene [(*E*)-**7**] or 1,2-di(4-pyridyl)ethane (1 mmol), and 3-bromopropylamine hydrobromide or 2-bromoethylamine hydrobromide (6 mmol) in anhydrous acetonitrile (20 mL) was refluxed under stirring for 13 h in the case of **2b–4b**, or for 140 h in the case of **2c**. After cooling to rt, the precipitate formed was filtered off, washed with anhydrous ethanol (4 × 50 mL) and chloroform (2 × 10 mL), and dissolved in water (20 mL). The solution was filtered and the filtrate was evaporated *in vacuo* to yield the corresponding tetrabromide of *N*,*N*′-di(ammonioalkyl) derivative as a yellow solid.

Method (b). The tetrabromide salt was dissolved in a mixture of ethanol (5 mL) and the minimum quantity of water with heating, and 70% aq. $HClO_4$ (0.6 mL) and ethanol (5 mL) were added to the hot solution. After cooling to 5 °C, the precipitate formed was filtered off and washed with ethanol (2 × 5 mL). The crystallization was repeated using half the amount of 70% aq. $HClO_4$ (0.3 mL) to give the corresponding tetraperchlorate of the *N*,*N*′-di(ammonioalkyl) derivative of the viologen analogue.

1-(3-Ammoniopropyl)-4-{(*E*)-2-[1-(3-ammoniopropyl)-4-pyridiniumyl]-1-ethenyl}pyridinium tetraperchlorate (2b). Obtained as a white solid in 72% overall yield; mp 301–304 °C (decomp.). IR ν/cm^{-1}: 3223, 3175, 3134 (NH). Lit. data: mp 293–295 °C (decomp.).[5a]

1-(2-Ammonioethyl)-4-{(*E*)-2-[1-(2-ammonioethyl)-4-pyridiniumyl]-1-ethenyl}pyridinium tetraperchlorate (2c). Obtained as a slightly brownish solid in 29% overall yield; mp 287–289 °C (decomp.). IR ν/cm^{-1}: 3187 (NH). ^{1}H NMR (DMSO-d_6, 30 °C) δ: 3.52 (br m, 4H, 2 CH_2NH_3), 4.80 (t, $J = 5.8$ Hz, 4H, 2 CH_2N), 8.15 (s, 2H, CH=CH), 8.40 (d, $J = 6.7$ Hz, 4H, 2H-3, 2 H-5), 9.04 (d, $J = 6.7$ Hz, 4H, 2 H-2, 2 H-6). Anal. calcld for $C_{16}H_{24}Cl_4N_4O_{16}$: C, 28.67; H, 3.61; N, 8.36; found: C, 28.57; H, 3.67; N, 8.31%.

1-(3-Ammoniopropyl)-4-{2-[1-(3-ammoniopropyl)-4-pyridiniumyl]ethyl}pyridinium tetraperchlorate (3b). Obtained as a white solid in 59% overall yield; mp 270–275 °C (decomp.). IR ν/cm^{-1}: 3231, 3188, 3137 (NH). ^{1}H NMR (D_2O, 25 °C) δ: 2.33 (m, 4H, 2 CH_2CH_2N), 3.06 (t, $J = 7.7$ Hz, 4H, 2 CH_2NH_3), 3.35 (s, 4H, 2 CH_2), 4.60 (t, $J = 7.7$ Hz, 4H, 2 CH_2N), 7.91 (d, $J = 6.5$ Hz, 4H, 2 H-3, 2 H-5), 8.69 (d, $J = 6.5$ Hz, 4H, 2 H-2, 2 H-6). Anal. calcld for $C_{18}H_{30}Cl_4N_4O_{16}$: C, 30.87; H, 4.32; N, 8.00; found: C, 31.07; H, 4.36; N, 8.04%.

1-(3-Ammoniopropyl)-3-{(*E*)-2-[1-(3-ammoniopropyl)-3-pyridiniumyl]-1-ethenyl}pyridinium tetraperchlorate (4b). Obtained as a white solid in 60% overall yield; mp 278–281 °C (decomp.). IR ν/cm^{-1}: 3231, 3187, 3149 (NH). ^{1}H NMR (CD_3CN, 25 °C) δ: 2.42 (m, 4H, 2 CH_2CH_2N), 3.14 (t, $J = 7.5$ Hz, 4H, 2 CH_2NH_3), 4.66 (t, $J = 7.5$ Hz, 4H, 2 CH_2N), 7.66 (s, 2H, CH=CH), 8.14 (dd, $J = 8.0$ Hz, $J = 6.3$ Hz, 2H, 2 H-5), 8.67 (d, $J = 6.3$ Hz, 2H, 2 H-6), 8.74 (d, $J = 8.0$ Hz, 2H, 2 H-4), 9.01 (s, 2H, 2 H-2). Anal. calcld for $C_{18}H_{28}Cl_4N_4O_{16}$: C, 30.96; H, 4.04; N, 8.02; found: C, 31.14; H, 4.11; N, 8.09%.

1-(3-Ammoniopropyl)-4-methylpyridinium diperchlorate (8). A mixture of 4-methylpyridine (0.30 mL, 3.1 mmol) and 3-bromopropylamine hydrobromide (1.02 g, 4.6 mmol) in anhydrous acetonitrile (20 mL) was refluxed under stirring for 4 h. The solvent was evaporated and the residue was washed with anhydrous ethanol (4 × 10 mL), dissolved in water (20 mL), and filtered. The mother solution was evaporated *in vacuo* to yield 0.50 g of 1-(3-ammoniopropyl)-4-methylpyridinium dibromide as a white solid. The dibromide was dissolved in a mixture of methanol (5 mL) and 70% aq. $HClO_4$ (1.0 mL) and the target diperchlorate was precipitated by adding diethyl ether (30 mL). The precipitate formed was filtered off and washed with a 5 : 1 benzene–ethanol mixture (2 × 10 mL). The crystallization was repeated using half the amount of 70% aq. $HClO_4$ (0.5 mL) to give **8** as a white solid (0.39 g, 36%); mp 150–152 °C. IR ν/cm^{-1}: 3228, 3181, 3137 (NH). ^{1}H NMR (D_2O, 25 °C) δ: 2.30 (m, 2H, CH_2CH_2N), 2.57 (s, 3H, Me), 3.03 (t, $J = 7.8$ Hz, 2H, CH_2NH_3), 4.56 (t, $J = 7.6$ Hz, 2H, CH_2N), 7.82 (d, $J = 6.0$ Hz, 2H, H-3, H-5), 8.59 (d, $J = 6.0$ Hz, 2H, H-2, H-6). Anal. calcd. for $C_9H_{16}Cl_2N_2O_8$: C, 30.78; H, 4.59; N, 7.98; found: C, 30.80; H, 4.64; N, 7.87%.

Preparation of supramolecular complexes (general procedure). An equimolar mixture of the bis(crown) stilbene **1b** and diammonium compound **2b–4b**, or **2c**, or a 2.3 : 1 mixture of **1b** and **2b**, or a 1 : 2.1 mixture of **1b** and **8** was dissolved in the minimum quantity of acetonitrile. The solution was slowly saturated with benzene through the gas phase at ambient temperature up to complete precipitation (visual control, for 3–5 days) and the precipitate formed was separated by decantation. The crystallization was repeated and the desired supramolecular complexes were obtained as fine-grained crystals in nearly quantitative yields. The composition of the complexes was confirmed by ^{1}H NMR spectra and elemental analysis.

Complex [1b · 9]. White crystals, mp 214–217 °C. IR ν/cm^{-1}: 3213, 3154, 3094 (NH). Anal. calcd. for $C_{46}H_{78}Cl_2N_2O_{20}$: C, 52.62; H, 7.49; N, 2.67; found: C, 52.74; H, 7.47; N, 2.66%.

Complex [1b · 2b]. Brown crystals, mp 260–263 °C. IR ν/cm^{-1}: 3170, 3126, 3063 (NH). Anal. calcd. for $C_{52}H_{76}Cl_4N_4O_{28}$: C, 46.37; H, 5.69; N, 4.16; found: C, 46.15; H, 5.72; N, 3.99%.

Complex [(1b)$_2$ · 2b]. Deep-brown crystals, mp 235–237 °C. IR ν/cm^{-1}: 3175 (NH). Anal. calcd. for $C_{86}H_{124}Cl_4N_4O_{40}$ × H_2O: C, 51.29; H, 6.31; N, 2.78; found: C, 51.26; H, 6.29; N, 2.72%.

Complex [1b · 2c]. Black crystals, mp 215–217 °C (decolor.) and >260 °C (decomp.). IR ν/cm^{-1}: 3170, 3127, 3050 (NH). Anal. calcd. for $C_{50}H_{72}Cl_4N_4O_{28}$: C, 45.53; H, 5.50; N, 4.25; found: C, 45.64; H, 5.75; N, 4.11%.

Downloaded by University of California - Los Angeles on 01 January 2013
Published on 11 May 2005 on http://pubs.rsc.org | doi:10.1039/B500667H

View Article Online

Complex [1b · 3b]. Yellowish crystals, mp 255–260 °C (decomp.). IR ν/cm^{-1}: 3171, 3130, 3088 (NH). Anal. calcd. for $C_{52}H_{78}Cl_4N_4O_{28} \cdot 2H_2O$: C, 45.09; H, 5.97; N, 4.05; found: C, 45.12; H, 5.94; N, 3.82%.

Complex [1b · 4b]. Yellow crystals, mp 185–190 °C. IR ν/cm^{-1}: 3175, 3151 (NH). Anal. calcd. for $C_{52}H_{76}Cl_4N_4O_{28} \times 1.5H_2O$: C, 45.46; H, 5.80; N, 4.08; found: C, 45.40; H, 5.97; N, 3.98%.

Complex [1b · (8)$_2$]. Yellowish crystals, mp 207–209 °C. IR ν/cm^{-1}: 3177, 3150 (NH). Anal. calcd. for $C_{52}H_{80}Cl_4N_4O_{28}$: C, 46.23; H, 5.97; N, 4.15; found: C, 46.25; H, 6.03; N, 3.96%.

Crystallographic study

Crystals of **1a**, **b** suitable for the X-ray diffraction experiment were grown by slow evaporation of CH_2Cl_2–hexane solutions. The single crystals were coated with perfluorinated oil and mounted on a Bruker SMART-CCD diffractometer (Mo-K$_\alpha$ radiation, ω scan mode, 0.3° frame, 15 s per frame). The structures were solved by direct methods and refined by full-matrix least-squares on F^2 in the anisotropic approximation for all non-hydrogen atoms. The hydrogen atoms were located from difference Fourier synthesis and refined in the isotropic approximation. The SHELXS-86 and SHELXL-97 software[18] were used for structure solution and refinement.

Crystal data for 1a. $C_{18}H_{20}O_4$, $M = 300.34$, monoclinic, $a = 8.9484(5)$, $b = 6.7152(3)$, $c = 12.4323(7)$ Å, $\beta = 92.500(3)°$, $V = 746.35(7)$ Å^3, $T = 120.0(2)$ K, space group $P2_1/c$ (no. 14), $Z = 2$, λ(Mo-K$_\alpha$) = 0.710 73 Å, 2775 reflections measured, 1064 unique ($R_{int} = 0.0278$) which were used in all calculations. The final R_1 and wR_2 were 0.0339 and 0.0844 for $I > 2\sigma(I)$, 0.0448 and 0.0892 for all data.

Crystal data for 1b. $C_{34}H_{48}O_{12}$, $M = 648.72$, monoclinic, $a = 42.778(2)$, $b = 9.0073(3)$, $c = 8.6096(3)$ Å, $\beta = 95.988(2)°$, $V = 3299.3(2)$ Å^3, $T = 100.0(2)$ K, space group $C2/c$ (no. 15), $Z = 4$, λ(Mo-K$_\alpha$) = 0.710 73 Å, 8379 reflections measured, 2900 unique ($R_{int} = 0.0661$) which were used in all calculations. The final R_1 and wR_2 were 0.0435 and 0.0839 for $I > 2\sigma(I)$, 0.0829 and 0.0949 for all data.

CCDC reference numbers 232849 and 238954.

See http://www.rsc.org/suppdata/nj/b5/b500667h/ for crystallographic data in CIF or other electronic format.

UV/Vis spectroscopy

Absorption spectra were recorded on a Specord-M40 spectrophotometer. Luminescence spectra were measured on a Shimadzu RF-5000 spectrofluorimeter. The complexation equilibria were studied in anhydrous acetonitrile (water $<0.01\%$) at 22 ± 2 °C. The complex formation constants were measured using the procedures described previously.[5b] The stability constants for the 1 : 1 D–A complexes between **1b** and **2b**–**4b** or **2c** are measured relative to the 1 : 1 complex of **1b** with 1,10-decanediammonium diperchlorate (log $K_1 = 7.58$, ref. 5*b*).

^{1}H NMR titration

The titration experiments were performed in CD_3CN solutions at 25 ± 1 °C. The concentration of acceptor (**2a**–**4a**, **2b**–**4b**, **2c**, or **9**) in solution was normally maintained at 1×10^{-3} M, and the concentration of donor (**1a** or **1b**) in the solution was gradually increased, starting from nothing. The highest donor/acceptor ratio was about 40. With the **1b/8** system, the concentration of **1b** was maintained at 1×10^{-3} M, and the concentration of **8** was varied from 0 to 6×10^{-3} M. The proton chemical shifts were measured as a function of the donor/acceptor ratio, and the complex formation constants were then calculated using the HYPNMR program.[14]

Acknowledgements

Support from the Russian Foundation for Basic Research (Projects 02-03-32286, 03-03-32178, and 03-03-32929), the INTAS (Grants 2001-0267 and YSF99-4051), the President of the Russian Federation (Grants MK-3666.2004.3 and MK-3697.2004.3), the Russian Science Support Foundation, the Russian Academy of Sciences, the Royal Society (L.G.K. and A.I.V.), the Royal Society of Chemistry for the RSC Journal Grants for International Authors (L.G.K. and A.V.C.), the EPSRC for a Senior Research Fellowship (J.A.K.H.), and the University of Umeå in the framework of a joint project of the University of Umeå and the Photochemistry Center of the Russian Academy of Sciences (CRDF, Grant RC0-872) is gratefully acknowledged.

References

1 (*a*) *Cation Binding by Macrocycles*, eds. Y. Inoue and G. W. Gokel, Marcel Dekker, New York, 1990; (*b*) R. M. Izatt, K. Pawlak, J. S. Bradshaw and R. L. Bruening, *Chem. Rev.*, 1991, **91**, 1721; (*c*) J.-M. Lehn, *Supramolecular Chemistry. Concepts and Perspectives*, VCH, Weinheim, 1995.

2 (*a*) H.-G. Löhr and F. Vögtle, *Acc. Chem. Res.*, 1985, **18**, 65; (*b*) P. de Silva, H. Q. N. Gunaratne, T. Gunnlaugsson, A. J. M. Huxley, C. P. McCoy, J. T. Rademacher and T. E. Rice, *Chem. Rev.*, 1997, **97**, 1515; (*c*) M. V. Alfimov and S. P. Gromov, in *Applied fluorescence in chemistry, biology, and medicine*, eds. W. Rettig, B. Strehmel, S. Schrader and H. Seifert, Springer-Verlag, Berlin, 1999, pp. 161–178; (*d*) B. Valeur and I. Leray, *Coord. Chem. Rev.*, 2000, **205**, 3.

3 (*a*) V. Balzani, A. Credi and M. Venturi, *Molecular devices and machines – A Journey in the Nano World*, Wiley-VCH, Weinheim, 2003; (*b*) *Molecular Switches*, ed. B. L. Feringa, Wiley-VCH, Weinheim, 2001; (*c*) J. D. Badjic, V. Balzani, A. Credi, S. Silvi and J. F. Stoddart, *Science*, 2004, **303**, 1845.

4 (*a*) S. Shinkai, in *Comprehensive Supramolecular Chemistry*, ed. J.-M. Lehn, Pergamon Press, New York, 1996, vol. 1; (*b*) S. P. Gromov and M. V. Alfimov, *Russ. Chem. Bull.*, 1997, **46**, 611; (*c*) V. Lokshin, A. Samat and A. V. Metelitsa, *Russ. Chem. Rev.*, 2002, **71**, 893; (*d*) D. G. Amirsakis, A. M. Elizarov, M. A. Garcia-Garibay, P. T. Glink, J. F. Stoddart, A. J. P. White and D. J. Williams, *Angew. Chem. Int. Ed.*, 2003, **42**, 1126; (*e*) M. V. Alfimov, O. A. Fedorova and S. P. Gromov, *J. Photochem. Photobiol., A*, 2003, **158**, 183.

5 (*a*) S. P. Gromov, E. N. Ushakov, A. I. Vedernikov, N. A. Lobova, M. V. Alfimov, Yu. A. Strelenko, J. K. Whitesell and M. A. Fox, *Org. Lett.*, 1999, **1**, 1697; (*b*) E. N. Ushakov, S. P. Gromov, A. I. Vedernikov, E. V. Malysheva, A. A. Botsmanova, M. V. Alfimov, B. Eliasson, U. G. Edlund, J. K. Whitesell and M. A. Fox, *J. Phys. Chem. A*, 2002, **106**, 2020.

6 (*a*) R. Foster, *Organic Charge-Transfer Complexes*, Academic Press, New York, 1969; (*b*) P. Bruni and G. Tosi, *Gazz. Chim. Ital.*, 1997, **127**, 435.

7 G. Lindsten, O. Wennerström and B. Thulin, *Acta Chem. Scand., Ser. B*, 1986, **40**, 545.

8 (*a*) C. Luis, M. M. Cid, R. Domingeuez, J. A. Seijas and M. C. Villaverde, *Heterocycles*, 1990, **31**, 1271; (*b*) P. Y. White and L. A. Summers, *Aust. J. Chem.*, 1977, **30**, 1153.

9 L. G. Kuz'mina, A. V. Churakov, J. A. K. Howard, A. I. Vedernikov, N. A. Lobova, A. A. Botsmanova, M. V. Alfimov and S. P. Gromov, *Crystallogr. Rep.*, 2005, **50**, 234 [Transl. from *Kristallografiya*, 2005, **50**, 266 (in Russian)].

10 S. P. Gromov, A. I. Vedernikov, E. N. Ushakov, L. G. Kuz'mina, A. V. Feofanov, V. G. Avakyan, A. V. Churakov, Yu. S. Alaverdyan, E. V. Malysheva, M. V. Alfimov, J. A. K. Howard, B. Eliasson and U. G. Edlund, *Helv. Chim. Acta*, 2002, **85**, 60.

11 M. V. Alfimov, S. P. Gromov, Yu. V. Fedorov, O. A. Fedorova, A. I. Vedernikov, A. V. Churakov, L. G. Kuz'mina, J. A. K. Howard, S. Bossmann, A. Braun, M. Woerner, D. F. Sears and J. Saltiel, *J. Am. Chem. Soc.*, 1999, **121**, 4992.

12 G. R. Desiraju, *Chem. Commun.*, 1997, 1475.

Published on 11 May 2005 on http://pubs.rsc.org | doi:10.1039/B500667H
Downloaded by University of California - Los Angeles on 01 January 2013

View Article Online

13 E. N. Ushakov, S. P. Gromov, A. V. Buevich, I. I. Baskin, O. A. Fedorova, A. I. Vedernikov, M. V. Alfimov, B. Eliasson and U. Edlund, *J. Chem. Soc., Perkin Trans. 2*, 1999, 601.
14 C. Frassineti, S. Ghelli, P. Gans, A. Sabatini, M. S. Moruzzi and A. Vacca, *Anal. Biochem.*, 1995, **231**, 374.
15 K. P. Butin, A. A. Moiseeva, S. P. Gromov, A. I. Vedernikov, A. A. Botsmanova, E. N. Ushakov and M. V. Alfimov, *J. Electroanal. Chem.*, 2003, **547**, 93.
16 A. M. Chippendale, G. McGeorge, R. K. Harris and C. M. Brennan, *Magn. Reson. Chem.*, 1999, **37**, 232.
17 A. Fisher, M. J. King and F. P. Robinson, *Can. J. Chem.*, 1978, **56**, 3068.
18 (*a*) G. M. Sheldrick, *Acta Crystallogr., Sect. A*, 1990, **46**, 467; (*b*) G. M. Sheldrick, *SHELXL-97, Program for the Refinement of Crystal Structures*, University of Göttingen, Germany, 1997.

Downloaded by University of California - Los Angeles on 01 January 2013
Published on 11 May 2005 on http://pubs.rsc.org | doi:10.1039/B500667H